Journal of Thermal Analysis and Calorimetry, Vol. 73 (2003) 183–190

PORE STRUCTURE OF GLASSES DERIVED FROM A LEACHABLE BOROSILICATE PRECURSOR
Thermoanalytical and BET methods

G. E. Romanos [3], *V. Kasselouri* [1*], *K. Beltsios* [2] *and N. K. Kanellopoulos* [3]

[1]NTU of Athens, Chem. Eng. Dept., Iroon Polytechniou 7, Zografou, Athens, Greece
[2]Department of Materials Science and Engineering, University. of Ioannina, Ioannina 45110, Greece
[3]NCSR DEMOKRITOS, Institute of Physical Chemistry, 15310 Ag. Paraskevi Attikis, Greece

(Received June 19, 2002; in revised form December 12, 2002)

Abstract

The aim of the present study was the pore structure characterization of porous glass derived from a leachable precursor. Two independent techniques were applied on this purpose. The interpretation of the results obtained by these techniques, i.e. thermoporometry and nitrogen porosimetry was indicative for their supplementary character in what concerns the calculation of pore size distributions. The experimental work described in this study gives an example for the monitoring of the compositional evolution of phase separating compact-glass precursors of porous glasses.

Keywords: BET method, borosilicate precursor, nitrogen adsorption, porous silica glass, porous structure, thermoporometry

Introduction

Knowledge of the surface area and pore size distribution is very important in catalysis and also in many other fields such as adsorbents, ceramics and membrane science. The determination of the isotherm of the physical adsorption of nitrogen, leads to the surface area of the sample by application of the well-known Brunauer–Emmett–Teller (BET) equation [1]. The calculation of the pore size distribution is performed by various methods based on the use of the Kelvin equation. A considerable amount of work has been carried out following Barret, Joyner and Halenda (BJH) [2] in order to derive pore size distributions and cumulative surface areas. The analysis by Broekhoff and De Boer [3] takes into account the shape of the pores and gives a good picture of the texture. Thermoporometry as a method for the calculation of the pore size distribution has been developed the last two decades. It has long been known that water held in small pores should freeze and melt at subzero temperatures. DSC curves associated with these phase transitions may be used to determine the porosity and pore size distribution of a particular sample. The characterization of the shape of the pores is made possible by the existence of a

* Author for correspondence: E-mail: vasrig@central.ntua.gr

1388–6150/2003/ $ 20.00
Akadémiai Kiadó, Budapest

hysteresis phenomenon between solidification and melting curves and is based on the definition of a shape factor, having previously excluded supercooling effects.

Experimental

Material preparation

The precursor used for the production of the samples was a mixture of 46.44% SiO_2-enriched natural quartz, 17.84% H_3BO_3, 3.92% Al_2O_3, 30% $Na_2B_4O_7 \cdot 10H_2O$ and 1.8% NaCl. The composition of the natural quartz is listed in Table 1. The approximate composition upon melting at 1400°C (which removes water and chlorine species) and subsequent quenching was: SiO_2: 61%, B_2O_3: 28.2%, Al_2O_3: 3.9%, Na_2O: 6.9%. Quenched samples were annealed at 630°C for times ranging from 15 min to 24 h. Subsequently, samples were crushed and leached with 2 M HNO_3 at 95°C for 2 h. Some of the samples were furthermore washed and leached with 0.5 M NaOH for 0.5 and 2 h. In this study, the pore structure of the annealed at 630°C samples was studied by thermoporometry (DSC) and nitrogen porosimetry (Quantachrome Autosorb-1 instrument).

Table 1 Composition of the natural quartz used for the precursor production

Oxide	Mass/%
SiO_2	96.14
Fe_2O_3	0.35
Al_2O_3	0.71
TiO_2	0.46
CaO	0.28
MgO	0.1
K_2O	0.045
Na_2O	0.034
R_2O_3 (unknown)	1.5

Sample preparation for thermal analysis

Two subsequent steps constituted the sample preparation. Degassing followed by saturation with deionised water. For this purpose a gas tight glass cuvette was constructed (Fig. 1). The cuvette consists of two distinguished parts connected with an Ultra Torr fitting (Cajon®). After degassing at high vacuum 10^{-5} mbar and at a temperature of 200°C for 24 h, the porous glass was saturated in water by opening of valve 1. Thus we avoided the contact of the sample with atmospheric air. Most of the excess water was taken off and a small amount of the sample (0.03–0.05 g) was transferred to an accurately weighted aluminium crucible (closed-type), for differential scanning calorimetry (T.A. Thermal Analyst 2100) under nitrogen atmosphere. Holes were tacitly opened on the crucible cover before weighting. The same crucible was

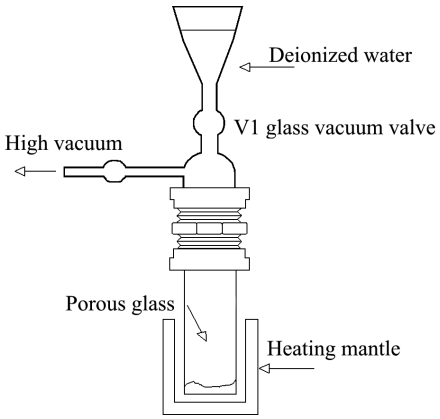

Fig. 1 Glass cuvette for the preparation for the saturation of samples with water

used as reference. Two sequential temperature programs were applied for differential scanning calorimetry. The first step included cooling at a rate of 1°C min^{-1} down to –50°C followed by heating (0.5°C min^{-1}) up to 20°C. In the second step a lower rate (0.1°C min^{-1}) was applied both for cooling and heating (–50 to 20°C). The aforementioned two steps procedure was followed to avoid supercooling effects [4]. After the experiments, the crucible containing the sample was degassed at high vacuum and temperature (200°C) and weighted, to calculate the real mass of the dry sample and absorbed water. DSC spectra were obtained for samples leached at different conditions listed in Table 2.

Table 2 Samples examined by thermoporometry and nitrogen porosimetry

Annealing time/h	Leaching with 2M HNO_3	NaOH 0.5 h	NaOH 2 h
0.25	DSC porosimetry	porosimetry	DSC porosimetry
0.5	–	–	DSC
1.5	DSC	–	DSC
2	–	–	DSC
3	DSC porosimetry	porosimetry	DSC porosimetry
4	porosimetry	porosimetry	DSC porosimetry
7	DSC	–	–
24	DSC porosimetry	porosimetry	DSC porosimetry

Sample preparation for nitrogen porosimetry

After leaching procedure the samples were washed with deionised water and preheated at 180°C in a solenoid oven with continuous flow of nitrogen. Their final degassing took place on the porosimeter outgassing stations at a temperature of 200°C and for a period of 24 h. Table 2 lists the samples to which nitrogen porosimetry was

contacted. Different P/P_0 points were acquired for samples which had not been treated with secondary leaching steps as they presented a microporous structure.

Results and discussion

Thermal analysis

The pore size distribution of samples was extracted by fusion DSC curves. Although a two-step cooling–warming procedure was followed, it was impossible to avoid supercooling effects. The fusion DSC curves of some of the samples are presented in Fig. 2. Assuming cylindrical geometry, the correlation between the fusion temperature depression (ΔT_F) and the pore radius (R_p), used for the extraction of the volumetric pore size distribution was the following [5]:

$$T_0 - T_F = \Delta T_F = \frac{1}{R_n} \frac{\gamma_{ls}}{\Delta S_F}$$

where T_0 (°C) the fusion temperature of bulk water, T_F (°C) the fusion temperature of water in pores, $1/R_n$ (nm^{-1}) the mean curvature radius of a circular cylinder, γ_{ls} ($N\ m^{-1}$) the free extension energy of solid–liquid interphase and ΔS_F ($J\ g^{-1}\ °C^{-1}$) the fusion entropy. The correlation of pore radius with the mean curvature radius $R_n=R_p-t$ (R_p the pore radius) in combination with the above equation gives:

$$R_p = -\frac{A}{\Delta T_F} + B$$

where $B=t$ (nm) the thickness of the adsorbed layer that doesn't undergo phase transformations [6]. The parameter A, includes physical-chemistry properties of water. A first step for the extraction of pore size distribution from the DSC curves was the determination of parameters A and B. Fusion DSC curves of controlled porous glass (CPG-82, CPG-130 and CPG-239) [7] have been used on this purpose. The plot of ΔT_F *vs.* R_p from the aforementioned analyses is presented in Fig. 3. Values of A=276.5 and B=3.95 were obtained from the slope and intercept of this plot. As it is already mentioned an adsorbed

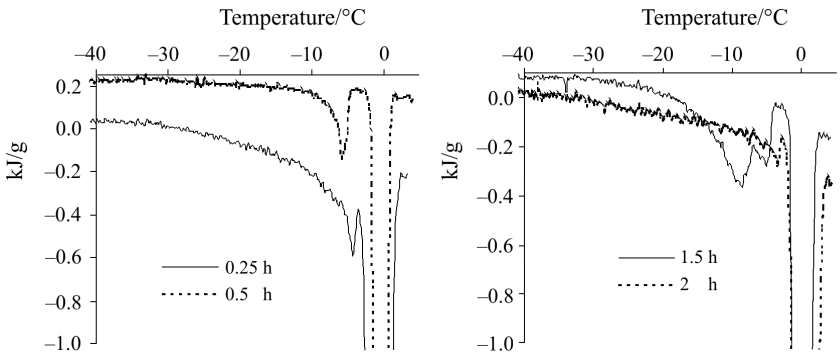

Fig. 2 Fusion DSC curves of samples, after the third step of leaching

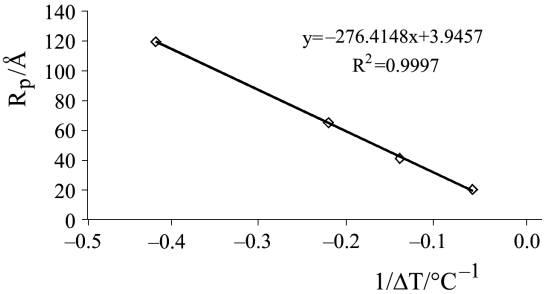

Fig. 3 Calculation of *A* and *B* parameters from CPG fusion DSC curves

water layer of thickness *B* doesn't undergo phase transformations. Thus in a pore of total volume V_p just a part of the held water V_p' fuses during warming and the apparent energy of transformation is given by $W_{app} = W_{th}' V_p' / V_p$ where the theoretical energy of transformation W_{th}' can be expressed in terms of the following relation [8]:

$$W_{th}' \approx T\Delta S_F \left(1 - \frac{d\gamma_{ls}\Delta T}{dT\gamma_{ls}} \right)$$

Taking into consideration the temperature dependence of ΔS_F and γ_{ls} for water [6] and interpreting the last two equations we have:

$$W_{app} = -0.155\Delta T^2 - 11.39\Delta T - 332$$

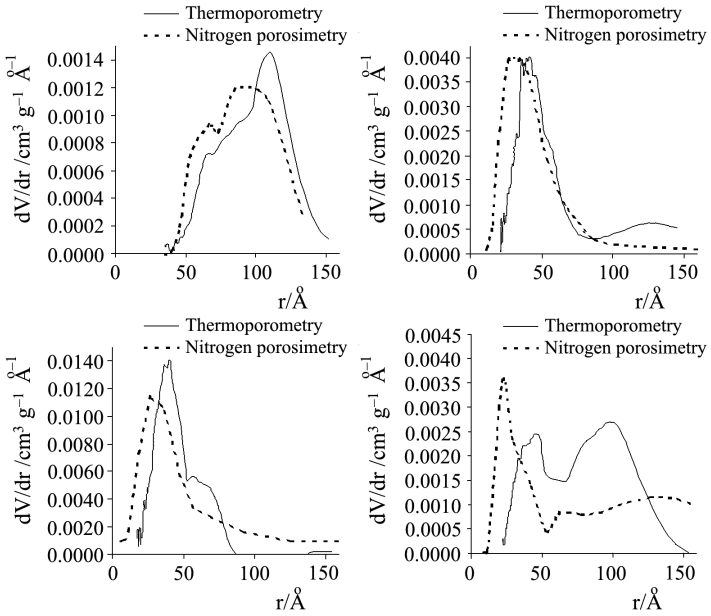

Fig. 4 Pore size distributions of samples after third leaching step; a – 4 h annealing; b – 24 h annealing, c – 1.5 h annealing, d – 3 h annealing

In the second step, fusion DSC curves were converted to the form dW/dt *vs*. t (time) by use of the applied heating rate (0.1°C min^{-1}). Consequently each DSC trace was divided in differential time increments dt and the area of the formed trapezoids was calculated according to the following equation:

$$E=\frac{\frac{\mathrm{d}W_{\mathrm{i}}}{\mathrm{d}t}t_{\mathrm{i}}+\frac{\mathrm{d}W_{\mathrm{i+1}}}{\mathrm{d}t}t_{\mathrm{i+1}}}{2}(t_{\mathrm{i+1}}-t_{\mathrm{i}})$$

The calculation of the differential volume dV_{p} that corresponds to a pore size dR_{p} was made after correction for the apparent energy W_{app}. The amount of bulk water was accurately calculated from the second endothermic peak (Fig. 2) and thus the mass of water held in the pores was calculated. All results were attributed per mass of adsorbed (intrapore) water and the curves of dV_{p}/dR_{p} *vs*. R_{p} were produced (Fig. 4). A comparison with pore size distributions extracted by nitrogen porosimetry, is also presented in this figure.

Nitrogen porosimetry

Nitrogen porosimetry isotherms are presented in Fig. 5. Useful results as for the total pore volume (mL g^{-1}), porosity ε, BET surface area A (m^2 g^{-1}) and mean radius R (Å) are extracted from the interpretation of the results and listed in Table 3. Pore size distributions derived by the BJH method [9] are presented in Fig. 4.

Table 3 Nitrogen porosimetry results

Annealing/h	Leaching conditions	V/mL g^{-1}	ε	A(BET)/m^2 g^{-1}	R(Å) (2×ε/A)
	HNO_3	0.206	0.301	422.3	9.78
0.25	NaOH 0.5 h	0.12	0.20	54.5	43.34
	NaOH 2 h	0.08	0.15	23.3	70.6
	HNO_3	0.1879	0.2820	229.03	16.41
3	NaOH 0.5 h	0.25	0.35	115.6	44.1
	NaOH 2 h	0.21	0.31	68.26	62.18
	HNO_3	0.2357	0.3300	539.3	8.74
4	NaOH 0.5 h	0.08	0.14	61.33	25
	NaOH 2 h	0.08	0.14	15.19	99.5
	HNO_3	0.2682	0.3591	496.16	10.81
24	NaOH 0.5 h	0.12	0.21	106.9	23.4
	NaOH 2 h	0.16	0.25	62.1	51.4

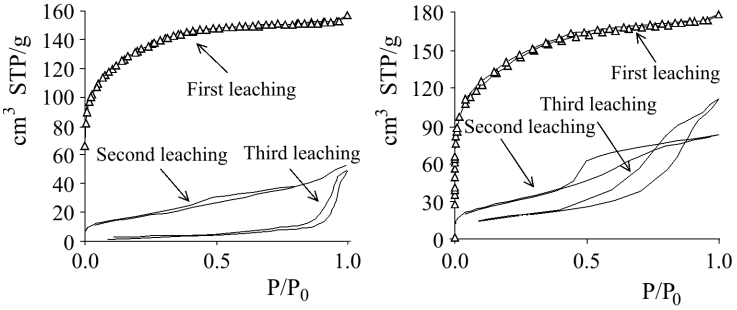

Fig. 5 Nitrogen (77 K) isotherms of samples; a – 4 h annealing; b – 24 h annealing

Supercooling effects

As mentioned previously, solidification DSC curves were not used in this study due to the impossibility to overcome supercooling effects. Supercooling is defined as a metastable situation in which the bulk water stays liquid at temperatures below its normal freezing point. Studies using X-ray diffraction have shown that the molecular arrangement in supercooled water becomes more and more ice-like as the temperature is lowered [10]. Calorimetric data indicate structural contributions to the differences between the specific heats of supercooled water and ice crystals and interpretation of these results leads to a conclusion that during supercooling, water molecules tend to form ice-like clusters incorporating six or more monomers [11]. The supercooling effect diminishes in the presence of a solid substrate as the water molecules are trapped in the ice lattice due to the effect of force field of the solid surface area. In the case of water trapped in porous solids supercooling can be avoided by warming up to 0°C, a sample that has already been cooled very fast and then applying a second cooling with slower rate. Thus the ice remaining in the porous system works as nucleation agent for the water held in the pores. However, for materials that contain constrictions, which seems to be our case, the aperture to the pore cavity is much smaller than the pore size and the water remains in a metastable phase inside the pore and behind the constriction. Two types of solidification DSC curves are possible for this category of samples. In the first type all the water supercools at a specific temperature and its characteristic for materials in which the temperature lowering for freezing is small, i.e. they have a large pore diameter or they are not efficient nucleators of the

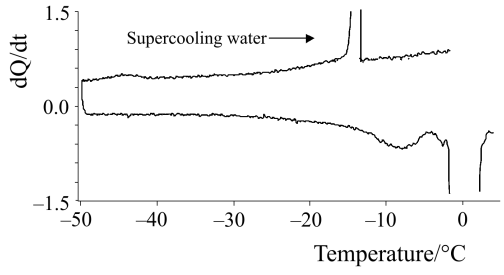

Fig. 6 Solidification and fusion DSC curves of a wet sample after third leaching step

ice phase. In the second type we have supercooling of water with ice in the saturated system. The DSC spectrum includes two exotherms from which the one at lower temperature represents equilibrium freezing of water in the small pore (nucleation being effected by the free ice in the system) and the other freezing of supercooled water in the larger pore (the ice phase being nucleated by the ice in the smaller pore). All of the samples examined presented the first type of solidification DSC spectrum (Fig. 6), indicating thus the presence of constrictions and large main pores.

Conclusions

The samples produced after the first leaching step, are characterized by a microporous structure with high surface area and a mean pore radius in the region of 10 Å (Table 3). The fusion DSC curves of these samples presented just a high endotherm around 0°C, which corresponds to the melting of the surface water. One of the possible mechanisms of solidification process is the formation of critical nuclei that have to reach a minimum size in order to grow. This size decreases with decreasing temperature but is also constricted by the size of the pore in which water is trapped. From the above it is obvious that we had to reach temperatures below –50°C in order to have freezing of water in the micropores of these particular materials. On the other hand the third leaching step (NaOH 2 h) had as effect the decrease of porosity by 20% with a simultaneous increase of the mean pore size. The above observation was indicative for the weak porous structure of the samples produced at an annealing temperature of 630°C. The value of the radii obtained through thermoporometry is superior to that given by the BJH method (Fig. 4), as BJH provides accurate information for the pore aperture [12]. This seems to point to the fact that all samples after the third leaching step presented a structure characterized by constrictions i.e. large cavities constricted by smaller orifices a notice also made by the impossibility to avoid supercooling effects.

References

1 S. Brunauer, P. H. Emmet and E. Teller, J. Amer. Chem. Soc., 60 (1938) 309.
2 E. P. Barrett, L. F. Joyner and P. H. Halenda, J. Amer. Chem. Soc., 73 (1951) 373.
3 J. C. P. Broekhoff and J. H. de Boer, J. Catal., 9 (1967) 8.
4 L. G. Homshaw, J. Coll. Inter. Sci., 84 (1981) 141.
5 C. Jallut, J. Lenoir, C. Bardot and C. Eyrad, J. Mem. Sci., 68 (1992) 271.
6 M. Brun, A. Lallemand, J. F. Quinson and C. Eyraud, Thermochim. Acta, 21 (1977) 59.
7 E. Robens, B. Benzler and K. K. Unger, J. Therm. Anal. Cal., 56 (1999) 323.
8 M. Brun, A. Lallemand, J. F. Quinson and C. Eyraud, J. Chim. Phys., 70 (1973) 973.
9 S. G. Gregg and K. S. Sing, Adsorption Surface Area and Porosity, 2nd Ed., Academic Press, New York 1982.
10 R. G. Dorsch and B. Boyd, U. S. N. A. C. A, Washington, Tech. Note 2532, 1951.
11 D. H. Rasmussen and A. P. Mackenzie, J. Chem. Phys., 59 (1973) 5003.
12 M. Iza, Polymer, 41 (2000) 5885.